

THEO & MUFN: Defending Earth Against the 2023 PDC Hypothetical Asteroid Impact

Melissa Buys^{a,1,*}, Jonathon L. Gabriel^{a,1}, Hannany Salehuddin^{a,1}, Raymond M. Squirini^{a,1}, Connor M. Wilson^{a,1}, Grace K. Zimmerman^{a,1}, Brent W. Barbee^{b,2}

^aUniversity of Maryland, College Park, MD, 20742, USA

^bNASA Goddard Space Flight Centre, Greenbelt, MD, 20771, USA

Abstract

Planetary defense is an emerging field among the aerospace community. As the rate of near-Earth object (NEO) discoveries increases, so too does the probability that we will discover a NEO on a collision course with Earth. This paper documents a planetary defense mission campaign design to defend against the hypothetical Earth impactor 2023 PDC. At its 90th percentile mass estimate, the asteroid could have a diameter of approximately 1120 m. The asteroid makes no close approaches until Earth impact and has the potential to affect over a billion people, depending on its actual size. This paper describes a mission campaign consisting of both reconnaissance and mitigation missions that will be deployed to neutralize the threat posed by the asteroid. The reconnaissance orbiter named THEO (Terrestrial Hazard Exploration Orbiter) will survey the asteroid to clarify its morphological, gravitational, and dynamical properties. This information will be used to inform the design of the subsequent mitigation mission. THEO will be designed to have a mission lifetime of 12 years which will enable it to observe the mitigation mission and confirm its success. Two 21-day launch periods have been identified that minimize post-launch ΔV requirements and include current launch vehicle capabilities. For the purposes of this paper, the mitigation mission has been designed assuming a geocenter impact for the 90th percentile mass estimate of the asteroid because a precise impact location and an accurate mass estimate will not be available until THEO reconnoiters 2023 PDC. The mitigation mission, named MUFN (Mitigation Using a Fission Nuclear device), will send three spacecraft to rendezvous with 2023 PDC and alter the asteroid's trajectory prior to Earth impact through a series of standoff nuclear detonations. The MUFN spacecraft are identical in design, each employing a hypergolic bi-propellant thruster. Each MUFN spacecraft launches on a SpaceX Falcon Heavy Expendable launch vehicle between 2028 and 2030 and carries four 340 kt nuclear explosive device (NED) equipped satellites, named BELASats (Bull's Eye, Later Asteroid Satellites (Sats)). The BELASats are designed to sequentially deploy, maneuver to an optimal standoff distance anti-parallel to the asteroid velocity vector, and detonate the NED to impart a change-in-velocity to the asteroid. After arrival at 2023 PDC, each MUFN spacecraft will station-keep above the asteroid. The NED-equipped BELASats will deploy from the MUFN spacecraft and maneuver 180 degrees out of phase from MUFN to the 'front' of the asteroid. Once there, each BELASat will detonate and impart 2.3 mm/s of velocity change to the asteroid. After the ablation debris has cleared and the detonation effectiveness has been assessed, MUFN will complete a single orbit around the asteroid to survey the blast site. After MUFN has completed its survey, it will release another BELASat. This process will repeat until all BELASats have been released by all MUFN spacecraft. All denotations will occur between 2029 and 2031. After all BELASats have detonated their NED payloads near the 2023 PDC asteroid to deflect its orbit, the asteroid will fly safely by Earth at a minimum altitude of 2000 km instead of colliding on October 22, 2036.

Keywords: Hypothetical Impactor, Orbiter, Nuclear, Reconnaissance, Mitigation

1. Introduction

Approximately 31,354 Near-Earth Objects (NEOs) have been discovered since 1970 [1]. Of these, 5% have been identified to have a non-zero Earth impact probability [2]. The National Near-Earth Object Preparedness Strategy and Action Plan (NNPSAP), written by the National Science and Technology Council, codifies NASA's efforts to detect and characterize NEOs [3]. There are various ways to increase preparedness for potential NEO impacts. The following five goals are listed in the NNPSAP:

1. Enhance detection, tracking, and characterization of NEOs.
2. Improve modeling, prediction, and information integration of NEOs.
3. Develop technologies for NEO mitigation missions.
4. Increase international preparedness and cooperation in preparation.
5. Strengthen impact emergency procedures.

It is not only the Earth at risk of NEOs' impact. A study on lunar impact flashes found that, seventy-nine lunar impact flashes were observed over 30 months [4]. The meteoroid masses that hit the moon in that period range from 0.7 to 8 kg and diameters between 1 and 20 cm [4]. There have been over 300 impacts on the surface of the moon since 2006 [5]. Furthermore, the estimated rate of crater creation on the surface of Mars is about 200,000 every year [6]. Finally, 188 impact craters have been confirmed on Earth [7]. The number of craters is significant given that Earth's atmosphere, vegetation, and active meteorological and geological weather processes obscure evidence of impacts.

The number of asteroid impacts on Earth and other bodies, such as the moon and Mars, further reinforces the importance of planetary defense. Currently, the Artemis program aims to send humans back to the moon with the aspiration of sending astronauts to Mars. For these explorations to be successful in the long term, it will be essential to develop the capability to mitigate the impacts on these two planetary bodies. Mitigation capabilities further motivate the need to invest in planetary defense mission design and demonstrations.

This paper will document a planetary defense mission campaign to defend against the hypothetical Earth impactor 2023 PDC. Figure 1 shows a patch designed for the mission campaign. The patch has the Earth presented by the University of Maryland Globe to which an asteroid is hurtling. The cat and dog represent the two spacecraft names, THEO and MUFN respectively. These were affectionately named after teammates' pets. Finally the six stars in the sky represent the six team members who worked together to design this mission campaign.



Figure 1: Mission Campaign Patch

2. 2023 PDC Information

The hypothetical Earth impactor 2023 PDC has been chosen as the NEO of interest for the mission design detailed in this paper. According to the scenario presented by CNEOS, the asteroid will be detected on 10 January, 2023, using the Dark Energy Camera (DECAM) on the Cerro Tololo Inter-American Observatory in Chile [8]. 2023 PDC is listed as a Potentially Hazardous Asteroid (PHA) because the initial assessment by the Minor Planet Center (MPC) reveals that the asteroid's orbit approaches Earth's orbit within 7.5 million kilometers and the asteroid is at least several hundred meters in size [8]. The design of a reconnaissance mission starts when the impact probability reaches 1% (3

*Corresponding author

Email address: mbuys@umd.edu (Melissa Buys)

¹Graduate Research Assistant, Department of Aerospace Engineering

²Flight Dynamics Engineer, NASA Goddard Space Flight Center

April, 2023), and the mitigation mission design starts when the impact probability reaches 10% (1 July 2023). There is a 100% probability of impact on 23 October, 2024 [8]. The impact is predicted to occur on October 22, 2036, roughly 13 years after discovery. Upon discovery, the asteroid is too distant for radar detection, so it is tracked using large optical telescopes.

The 10th and 90th-percentile mass estimate (Table 1) of 2023 PDC can be inferred from the asteroid's brightness, estimated using ground telescopes. The asteroid's absolute magnitude is estimated to be $H = 19.4 \pm 0.3$, which indicates that it is relatively large. More information is needed to determine the mass and diameter of the asteroid with higher accuracy. It is also unclear whether 2023 PDC is part of a binary system or whether the body is an S, M, or C-type asteroid.

Table 1: 2023 PDC Properties

Property	Mass Percentile	
	10th	90th
Porosity	0.32	
Bulk Density [g/cm^3]	1.802	
Mass [kg]	2.42×10^{10}	1.32×10^{12}
Diameter [m]	295	1119

2023 PDC has an almost circular orbit that is 0.9 au from the Sun at perapsis and 1.07 au at apoapsis, the orbit also has an inclination of approximately 10 degrees. 2023 PDC's orbital period is 359 days, and as a result of its orbital period, it will slowly catch up to Earth until its impact in 2036. Propagation of 2023 PDC yields that, post-discovery and until impact, the Earth and asteroid are out of phase with a long synodic period. As a result of this phase difference, there are no close approaches to Earth until impact. Figure 2 shows the orbits of the two bodies along with their possible impact position at the node where the orbits cross.

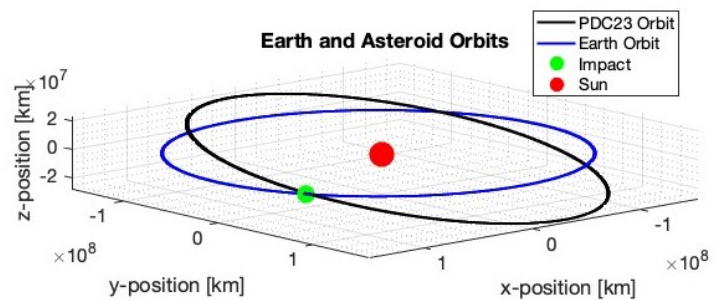


Figure 2: Earth and 2023 PDC Orbits

3. Terrestrial Hazard Exploration Orbiter: THEO

3.1. Objectives

Knowledge of the orbital and physical properties of 2023 PDC is essential in the design of a mitigation mission. The uncertainties in crucial properties such as orbital state and mass are considerable during the early stages of 2023 PDC detection and observations. In situ reconnaissance of the asteroid may be the only means of reducing key uncertainties in asteroid properties to enable the mitigation mission to be carried out reliably. Effective mitigation mission planning is enabled earlier by obtaining high-fidelity estimates of the asteroid's mass, size, and composition. Furthermore, these properties would enable accurate modeling of impact consequences to inform disaster response planning and a cost-benefit analysis for mitigation vs. accepting the impact. Essential factors in designing the mitigation mission include rotation rate, material, and internal composition [9]. Sending an orbiter to 2023 PDC will provide additional insight into the diameter, bulk density, rotation period, rotational acceleration, and material composition, among other things.

The Terrestrial Hazard Exploration Orbiter, THEO, will be a reconnaissance orbiter that will rendezvous with 2023 PDC. It will be sent to 2023 PDC three to four years before a mitigation mission is launched. An orbiter was chosen over a flyby spacecraft due to the wide range of the estimated mass and diameter values for 2023 PDC. The orbiter will gather essential data about the physical and elemental properties of the asteroid. Furthermore, it will assess the extent of threat mitigation with a higher degree of confidence than a ground-based observer. Figure 3 shows the nominal timeline for the reconnaissance and mitigation missions in 13 years to ensure the elimination of the threat posed by 2023 PDC before Earth's impact.

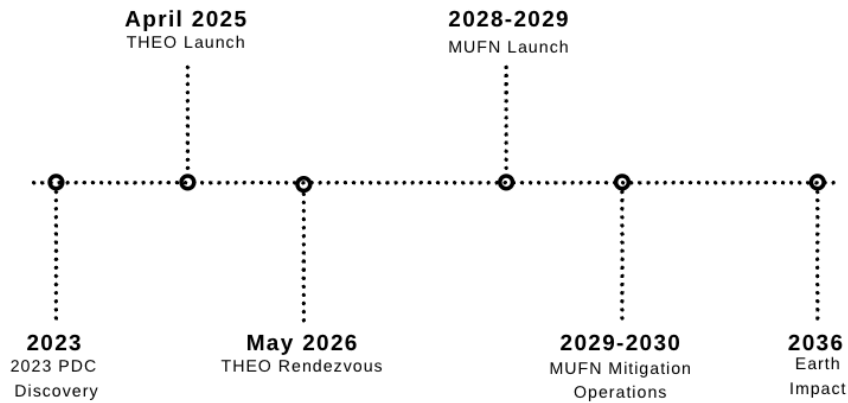


Figure 3: 13-Year Mission Timeline

3.2. Requirements

The mission requirements for THEO are presented below in Table 2. The requirements enable THEO to be launched as soon as possible and send back critical data about 2023 PDC to inform the mitigation mission.

Table 2: Reconnaissance Mission Requirements

Number	Requirement
R1	THEO shall launch no later than December 2025.
R2	THEO shall arrive at 2023 PDC no later than two years after launch.
R3	THEO shall have a wet mass of no more than 2,000 kg.
R4	THEO shall study the morphological characteristics of 2023 PDC.
R5	THEO shall study the gravitational and dynamical properties of 2023 PDC.
R6	THEO shall study the elemental composition of 2023 PDC.
R7	THEO shall image the space around 2023 PDC.
R8	THEO shall have a mission lifetime of 12 years.

3.3. Spacecraft Design

This section will outline the instruments that will be present on THEO. The orbiter will consist of commercial off-the-shelf (COTS) and build-to-print components as much as possible. This strategy ensures that THEO can be built and launched according to requirement **R1**.

3.3.1. Scientific Instruments

THEO will consist of five scientific instruments. These instruments were selected for THEO because they have proven effective on previous orbiter missions to asteroids [10, 11, 12, 13]. Table 3 shows which requirements are fulfilled by each instrument.

Table 3: Requirements satisfied by chosen instruments.

Instrument	Requirement
Imagers (Visual and Infrared)	R4, R7
Spectrometer	R6
Laser Altimeter	R5, R6
X-band Transponder	R5, R6

A combination of optical and infrared cameras will be used to image 2023 PDC upon approach and while in orbit. These imagers will determine the shape of the object and specific features on its surface. Using commercially available solutions means that THEO will have two imagers on board which will cover infrared and visual wavelengths. These instruments will enable visual data of 2023 PDC to be recorded from at least 1,000 km altitude, which will be THEO's maximum loiter altitude while it observes the mitigation mission.

THEO will have spectrometers to cover a wide range of spectral wavelengths. The first will be a visual and infrared spectrometer. This instrument will cover wavelengths from 0.25 - 5 microns [11]. The visual and infrared spectrometer will measure the sunlight reflected from 2023 PDC to determine the abundance of surface materials [10]. Next, THEO will have an x-ray spectrometer. This instrument will detect x-rays in the 0.5 - 5 keV range [14]. The x-ray spectrometer on THEO will be a build-to-print spectrometer from the OSIRIS-REx mission because the technology has already proven to be successful for an asteroid reconnaissance mission [14, 15, 16]. X-rays are emitted from rock-forming and radioactive elements on the surface of the asteroid [10, 11, 12, 13]. Knowing the abundance of elements on the surface of 2023 PDC will inform the mitigation technique used for the mitigation mission. The fourth instrument on THEO will be a laser altimeter that will measure the distance from the spacecraft to the asteroid by measuring the time it takes for a burst of laser light to travel from the spacecraft to the asteroid's surface and back [10]. The laser altimeter will be used to construct a shape model of 2023 PDC [10, 11]. This instrument will determine the topographical features and gravitational attraction of 2023 PDC [17]. Finally, an x-band transponder that will form part of the communications suite can measure the Doppler shift from the spacecraft's radial velocity vector component relative to the Earth [10]. This measurement will be used to determine the asteroid's gravity field [11, 10, 12, 13]. This gravity investigation will aid in determining the mass, principal axes, rotational axes, and moments of inertia of 2023 PDC [11, 12]. Once a shape and gravity model of 2023 PDC has been put together, it will be possible to characterize the crust and mantle density variations of 2023 PDC [11]. The transponder will allow connection to NASA's Deep-Space Network (DSN) for communication purposes.

3.3.2. Propulsion System

THEO will be equipped with four 445N MON3-MMH bi-propellant thrusters for high-thrust applications and deep space maneuvers (DSMs). Along with the high-thrust engines, THEO will also have twelve 1N mono-propellant hydrazine thrusters for attitude control and small thrust maneuvers. THEO will have two 700-1108 liter tanks for the bi-propellant system. The 1N mono-propellant thrusters will have a separate hydrazine fuel tank. The thruster properties are presented in Table 4.

Table 4: Thruster Properties

Thruster	Propellant	Specific Impulse (s)	Thrust Range (N)	Minimum Impulse Bit (N-s)	Mass (kg)
R-4D-15	MMH/MON3	320 - 322	378 - 511	35.6	3.5
MR-103G 1N	Hydrazine	202 - 224	0.19 - 1.13	0.013	0.3

3.4. Mass Summary

Table 5 presents a summary of the subsystem masses for THEO. THEO's total dry mass is 741 kg. Using an Isp of 320 s and the mission ΔV of 2.6 km/s, the interplanetary travel propellant is calculated as 1242 kg. Finally, with an Isp of 202 s and a ΔV of 30 cm/s, the propellant needed for proximity operations at 2023 PDC is calculated as 1 kg. The total propellant needed for the THEO mission is 1243 kg. THEO's wet mass will be 1984 kg which satisfies requirement R3.

Table 5: THEO Subsystem Mass Summary

Subsystem	Mass (kg)	% Margin
Science Instruments	122	75
Structure	155	25
Thermal	48	50
Power	116	35
TT&C	50	75
GNC	43	30
Propulsion	207	25
Interplanetary Travel Propellant	1242	30
2023 PDC Proximity Operations Propellant	1	400
Total Dry Mass	741	-
Total Propellant Mass	1243	-
Total Spacecraft Mass	1984	-

3.5. Trajectory

Potential Earth launch and 2023 PDC arrival dates were investigated alongside various times-of-flights (TOF) using a Type II Lambert solution. To begin the investigation, launch dates from 01/01/2025 to 01/01/2028 and arrival dates from 02/01/2025 to 02/02/2028 were considered. The trajectories were further constrained by considering launch energy (C3) estimates less than $70 \text{ km}^2/\text{s}^2$, the limit according to THEO **R3** requirement, and current launch vehicle technology [18]. Furthermore, the declination launch asymptote (DLA) was constrained between -57 and 57 deg to account for Kennedy Space Center launch capabilities.

Following the initial search, all launch dates were further constrained to 2025 and arrival dates up to Dec. 2026 based on the THEO **R1** and **R2** requirements. The arrival date constraint was enforced to allow adequate time to gather and process scientific data for the mitigation mission. Following the constrained search, two launch periods of twenty-one days each were identified within 2025, with arrival dates of 05/26/2026 (Figure 4) and 10/08/2026, respectively.

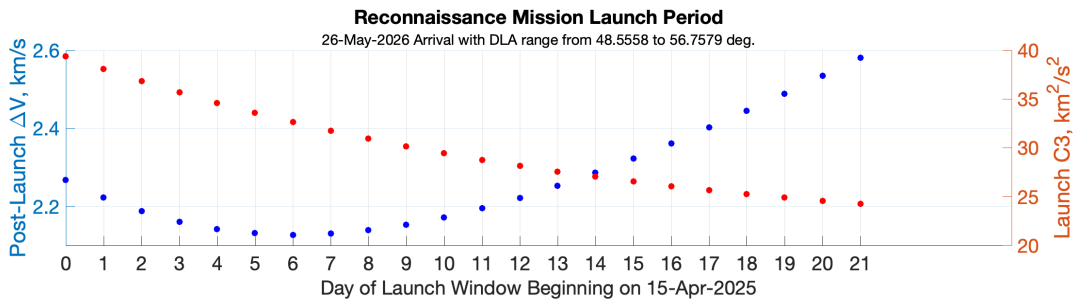


Figure 4: Launch Period for Reconnaissance Mission

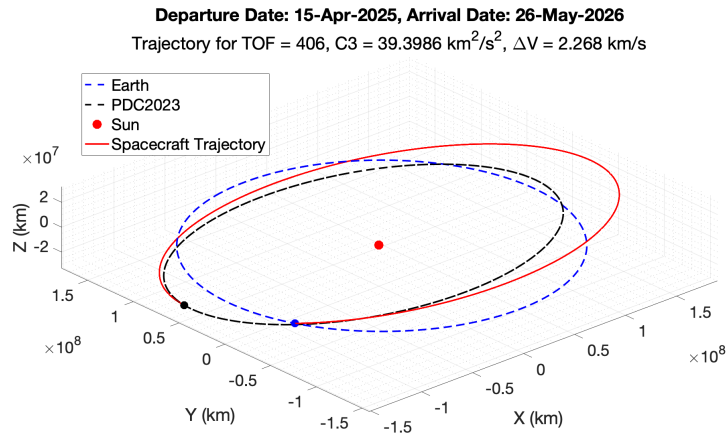


Figure 5: Trajectory for First Day of Launch Period

3.5.1. Proximity Operations

Once THEO has reached 2023 PDC, it will rendezvous with the asteroid and conduct various orbits to collect precise data. The different instruments onboard THEO will be most accurate at different altitudes above 2023 PDC [10, 11]. A series of DSMs will be performed one week, two days, and 12 hours from the initial estimated arrival. At a distance of 7km from PDC, THEO will perform a maneuver to transfer into an elliptical orbit to survey the PDC gravity. From this point, THEO will begin its survey and mapping orbits. The process begins with a 19km radius circular survey orbit, followed by a 6.5km high altitude mapping orbit. After this point, THEO will transfer into a 1.75km low-altitude orbit, followed by a 1,000km observation orbit. The observation orbit radius was determined based on MUFN requirements with THEO acting as a point of redundancy for observing the mitigation detonations. The proximity operations, transfer types, ΔV , and thruster burn time requirements are detailed in Table 6.

Table 6: Proximity Operations Maneuvers

Trajectory Description	Transfer Type	Burn Time (s)	ΔV
Deep Space Maneuver 1	Reduction in Speed	18 min	1.0 km/s
Deep Space Maneuver 2	Reduction in Speed	10 min	0.75 km/s
Deep Space Maneuver 3	Reduction in Speed	8 min	0.75 km/s
Elliptical GM Survey	Elliptical capture orbit maneuver	1 min	0.1 km/s
Survey Orbit	Circularize orbit, Hohmann transfer to 19km	3 sec	8.98 cm/s
High Alt. Mapping Orbit (HAMO)	Hohmann transfer to 6.5km	0.15 sec	4.19 cm/s
Low Alt. Mapping Orbit (LAMO)	Hohmann transfer to 1.75km	0.26 sec	7.77 cm/s
MUFN Observation Orbit	Hohmann transfer to 1,000km	0.28 sec	1.21 m/s
THEO 5-Yr Station Keeping	-	-	0.053 km/s

During the initial survey orbit, THEO will spend five Earth days imaging 2023 PDC. The visual and infrared spectrometer will complete low-resolution mapping of the asteroid at this time [11]. The survey period is also when the region around 2023 PDC will be searched for debris or secondary bodies. After the survey orbit, THEO will spend 30 Earth days in the high altitude-mapping orbit (HAMO) [11]. This lower orbit is where most of the mapping of the asteroid’s surface will take place. The imagers and visual-and-infrared spectrometer will collect high-resolution data in the HAMO. THEO will spend in 60 Earth days in the low altitude-mapping orbit (LAMO) [11]. The gamma-ray spectrometer and laser altimeter instruments will gather data in this orbit. The asteroid’s gravity field will be measured in both HAMO and LAMO. In conjunction with the measurements from the survey orbit, these measurements can be used to construct a model of the gravity field of 2023 PDC to inform the mitigation mission. Figures 6 and 7 are graphical representations of how the arrival and proximity operations around 2023 PDC will look, with 2023 PDC represented by 101955 Bennu.

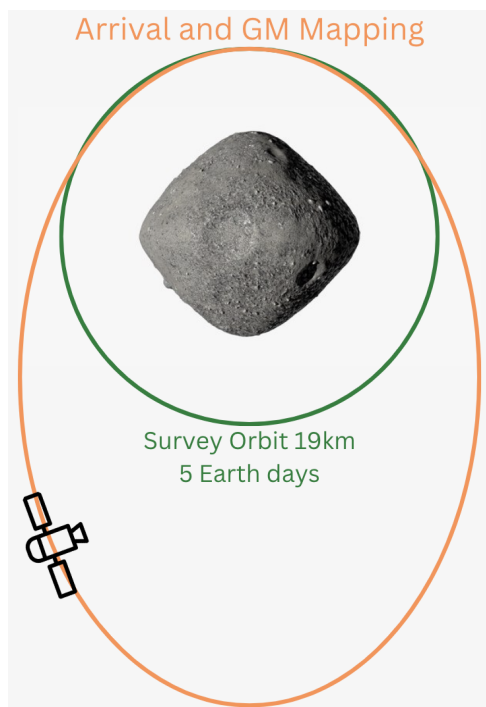


Figure 6: THEO Arrival Orbits

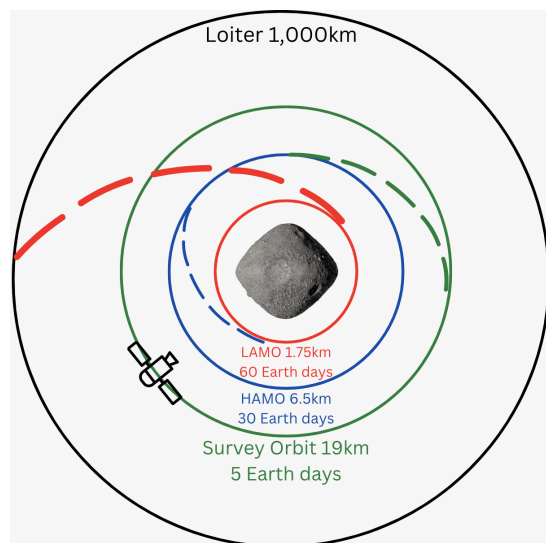


Figure 7: THEO Proximity Operation Orbits

3.6. THEO Risks

Figure 8 presents the risk chart for THEO, and the risk descriptions are presented in Table 12. Various methods will be employed to attempt to mitigate these risks. As previously mentioned, COTS components will be used to facilitate THEO’s short development time. Furthermore, additional iterations

of already selected components can be done to ensure their delivery as soon as possible. Using COTS components will also ameliorate budgetary constraints since money does not have to be spent on significant technology development. Two THEO spacecraft will be built to account for risks 2 - 5, 7, and 8. If there is a critical failure of the first THEO spacecraft, the second can be launched in the backup launch window. Finally, critical spacecraft components will have duplicates to ensure that there are backup components on board should the primary components fail.



Figure 8: THEO Risk Chart

Table 7: THEO Risk Factors

Risk #	Description
1	Short development phase
2	Launch vehicle failure
3	Critical spacecraft component failure
4	Rendezvous difficulties
5	Orbit difficulties
6	Budgetary constraints
7	Separation system from launch vehicle
8	Failure after the science mission

4. Mitigation Using a Fission Nuclear device: MUFN

4.1. Mitigation Mission Requirements

After the confirmation of the characteristics of the asteroid by THEO, a standoff nuclear detonation mitigation mission will be sent to neutralize the threat posed by 2023 PDC. The mitigation mission to 2023 PDC has been named MUFN (pronounced as Muffin): **Mitigation Using a Fission Nuclear device**. Table 8 presents the requirements of the mitigation mission.

Table 8: Mitigation Mission Requirements

Number	Requirement
M1	MUFN shall neutralize the threat posed by 2023 PDC.
M2	MUFN shall launch no later than December 2029.
M3	MUFN shall arrive at 2023 PDC no later than two years after launch.
M4	MUFN shall have a wet mass of no more than 5000 kg.

The proposed timeline for MUFN will follow a five-year schedule. It will have a five-year development phase and a maximum two-year lifetime after launch. The asteroid mitigation mission has been designed to successfully neutralize the threat posed by the 90th percentile parameters of 2023 PDC, found in Table 1. Designing against the upper asteroid mass estimates ensures a more robust initial design phase of the mitigation mission by first preparing for the most challenging conditions and later down-scaling the designs based on the data returned by the THEO reconnaissance mission if required. The 90th percentile parameters were also selected to prepare for the scenario in which THEO fails and the only available data is sourced from Earth ground-based telescopes.

4.2. MUFN Concept of Operations

The MUFN CONOPS is split into three primary mission phases: arrival phase, detonation phase, and observation phase. Figure 9 provides CONOPS graphics to augment this discussion. Functionally, the complete MUFN spacecraft system consists of five independent spacecrafts. The MUFN spacecraft is the "bus" that transports four BELASats across inter-planetary space from Earth orbit to the target asteroid 2023 PDC. The BELASats are self-sufficient small satellites responsible for housing and delivering the individual NEDs to their detonation positions.

In the arrival phase the MUFN spacecraft, with its four attached BELASats, will enter the sphere of influence of 2023 PDC and will reach a pre-determined station-keeping altitude above the asteroid. The specific station-keeping altitude that MUFN will occupy will be 1.75 kilometers. Once MUFN is stable at this station-keeping altitude, the next phase of operations can begin. The next phase, detonation, involves sequential separation of each of the four BELASats from the MUFN bus spacecraft. Each BELASat spacecraft will separate from the MUFN bus spacecraft, enter an elliptical transfer orbit, and arrive at the opposite side of 2023 PDC relative to MUFN. Once each BELASat has arrived on the opposite side of the asteroid, it will orient itself to an optimal standoff distance relative to the asteroid's surface and detonate. This process will be completed for each of the four BELASats. It is important to note that MUFN will be on the opposite side of the asteroid relative to the BELASat during each detonation and thus shielded from the majority of the detonation effects. After the detonation the final phase, observation, takes place. The MUFN spacecraft will observe changes in 2023 PDC's orbital state, gauging the effectiveness of each blast. THEO will also be able to observe the detonation from its safe observation altitude. The MUFN and THEO observations will gauge each nuclear detonation's effectiveness before another BELASat is launched. This allows for tuning of each detonation which will be discussed in future sections. It is also important to note that to fully mitigate the threat posed by 2033 PDC, three MUFN spacecraft (delivering 12 total BELASats) will be launched. The justification for these values will be provided in future sections. A reserve MUFN spacecraft, carrying four additional BELASats, will be launched in case it is needed for any reason.

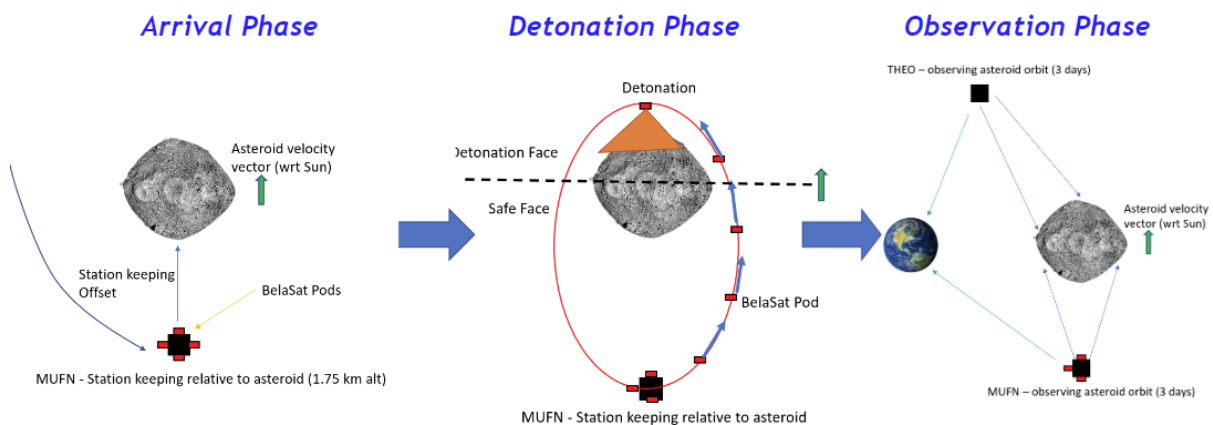


Figure 9: MUFN concept of operations visualization

4.3. NED Design

A standoff nuclear detonation operates by detonating a NED at a set distance above the surface of the target asteroid and bombarding the asteroid's surface with radiation and high-energy particles. A thin layer of the surface material is vaporized on the magnitude of several centimeters and outgassing occurs from the ablation process. The resulting momentum transfer imparts a change in velocity on the target asteroid, altering its orbital period and thus changing the object's trajectory [19]. Since nuclear detonation occurs in the vacuum of space, there will not be a post-detonation blast wave as with Earth-based nuclear weapons. Similarly, there will be an absence of thermal radiation since there is no air for the blast wave to heat [20]. All imparted velocity changes result from the outward expansion of radiation from the point of detonation.

The amount of imparted ΔV required to successfully prevent Earth impact informs the design of the individual NEDs. Using the NASA CNEOS NEO deflection application, a first-order estimate of ΔV required to deflect 2023 PDC was built as a function of the deflection time. The parameters placed into the NEO deflection app were tuned to the 90th percentile characteristic values given, resulting in a mass value matching the 90th percentile expected for 2023 PDC. Figure 10 shows this data plotted and provides a convenient polynomial curve fit that estimates the required deflection ΔV as a function of deflection time, measured in years before impact. Per mitigation requirement **M2** (deflect the asteroid no later than seven years before projected Earth impact), the minimum required ΔV imparted to the asteroid for successful deflection is 25 mm/s [21].

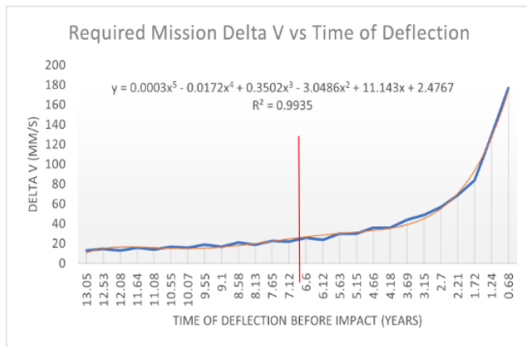


Figure 10: Required Imparted ΔV vs Time Before Earth Impact for Successful Deflection

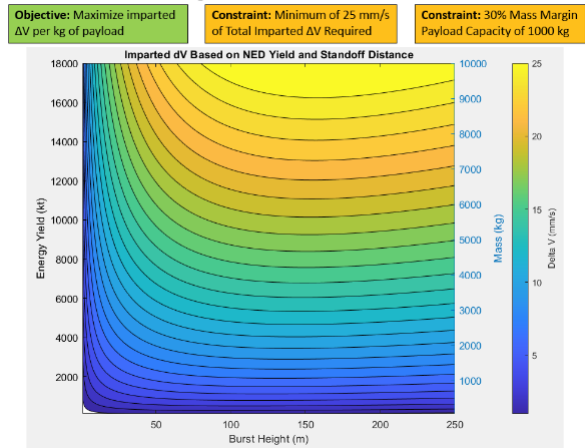


Figure 11: Imparted ΔV Based on NED Yield and Standoff Distance

A study into the effects of NED yield and standoff distance from the asteroid's surface on the total imparted ΔV to the asteroid was performed using the methodology outlined by Managan et al. in *Near Earth Object Deflection Formulae* [22]. Preliminary testing analyzed energy yields up to 18 Mt, and standoff distances up to 250 m above the asteroid's surface. The imparted ΔV values at the optimal distances over this range of data are shown in Figure 11. Also included in Figure 11 are the associated device masses for each energy yield for payload design purposes. All NED mass calculations were performed assuming a 1 kg NED outputs an energy yield of 1.8 kt. Next, an optimization study was performed on the data set to maximize the imparted ΔV per kilogram of NED payload. After assuming a 30 percent mass margin on the MUFN mitigation spacecraft, a maximum payload of 1000 kg was established, and the constraint was integrated into the system optimization study. Additionally, the system was constrained to ensure that the collective NED detonations impart a minimum of 25 mm/s of ΔV .

The findings of the optimization study highlight the value in delivering multiple lower-yield NEDs with each launch rather than relying on singular high-yield NEDs to impart the required ΔV . Figure 12 analyzes the maximum imparted ΔV values, which would occur at some optimal standoff distance across the full range of NED yields. The two plots verify the trend that the imparted ΔV per kilogram of NED mass is higher for lower yields. Thus, under the given optimization constraints, it is highly beneficial to target sub-500 kt NED yields.

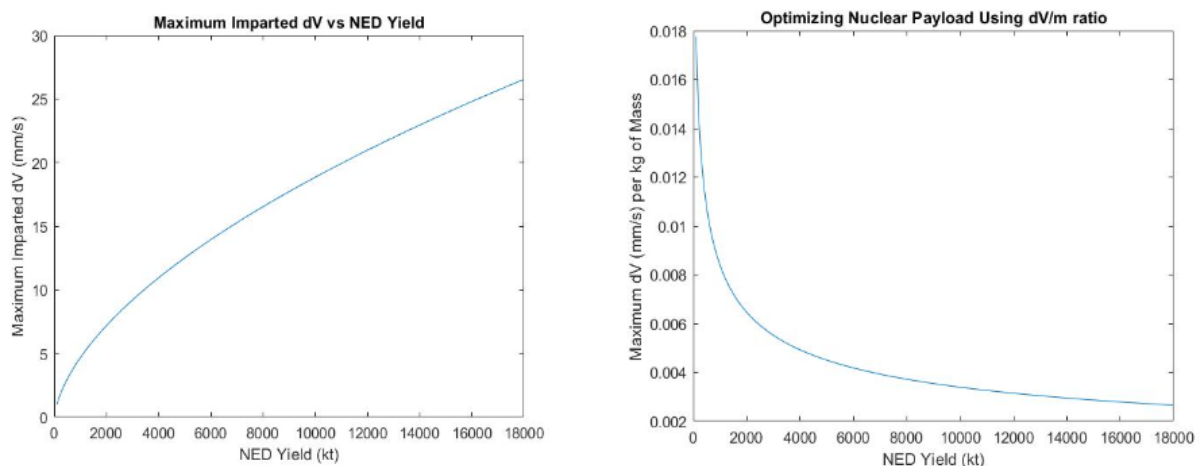


Figure 12: Payload Optimization Considerations

Having established the value of using lower-yield NEDs, the next step in the optimization process is determining the number of NEDs that can be transported on each launch vehicle. An additional constraint of a maximum of three primary SpaceX Falcon Heavy Expendable launches has been added.

This additional constraint ensures that all launch vehicles, which include one redundant secondary Falcon Heavy Expendable, can be prepped and launched within the selected launch windows. Figure 13 shows select results from the complete optimization study for one to three primary Falcon Heavy Expendable launches. The individual NED yield, the individual and total imparted ΔV , the NED mass, the remaining Falcon Heavy payload capacity after factoring in the NEDs, and the optimal standoff distance is included for each option. Given the system constraints, it is not possible to successfully deflect 2023 PDC with a single Falcon Heavy Expendable launch. Mission success is possible with two launches; however, a minimum payload of twelve 110 kt NEDs would need to be transported with each launch. This option was eliminated to reduce potential points of failure and reserve payload capacity for the hardware associated with the MUFN spacecraft bus responsible for delivering the NEDs to 2023 PDC.

The chosen NED design is highlighted in green in Figure 13. Each MUFN mitigation spacecraft bus will launch on a Falcon Heavy Expendable and transport four 340 kt NED-equipped satellites, named BELASats, to 2023 PDC. Upon detonation at an optimal standoff distance of 99 m, each individual BELASat will impart 2.32mm/s of ΔV . Three Falcon Heavy Expendable launches will be required to impart a total ΔV of 27.8 mm/s and clear the 25mm/s requirement. A fourth Falcon Heavy Expendable will launch a redundant MUFN mitigation vehicle to account for potential technical difficulties or hardware failures. The redundant vehicle also covers the scenario where more ΔV is required to deflect 2023 PDC than initially anticipated.

NED Options for Successful Deflection with 1 Falcon Heavy Launch Vehicle							
Individual NED Yield (kt)	Number of NEDs per FH	Imparted ΔV per NED (mm/s)	Total Imparted ΔV per FH (mm/s)	Individual NED Mass (kg)	Total NED Mass per FH (kg)	Remaining FH Payload Capacity (kg)	Optimal NED Standoff Distance (m)
Not Possible							
NED Options for Successful Deflection with 2 Falcon Heavy Launch Vehicles							
80	15	0.84	12.56	44.44	666.67	333.33	63.00
85	15	0.88	13.13	47.22	708.33	291.67	65.00
90	14	0.91	12.79	50.00	700.00	300.00	66.00
95	14	0.95	13.30	52.78	738.89	261.11	68.00
100	13	0.99	12.83	55.56	722.22	277.78	69.00
105	13	1.02	13.29	58.33	758.33	241.67	70.00
110	12	1.06	12.69	61.11	733.33	266.67	71.00
NED Options for Successful Deflection with 3 Falcon Heavy Launch Vehicles							
125	8	1.16	9.28	69.44	555.56	444.44	75.00
130	7	1.19	8.35	72.22	505.56	494.44	76.00
160	7	1.38	9.67	88.89	622.22	377.78	81.00
165	6	1.41	8.47	91.67	550.00	450.00	82.00
205	6	1.64	9.85	113.89	683.33	316.67	87.00
210	5	1.67	8.35	116.67	583.33	416.67	88.00
290	5	2.08	10.41	161.11	805.56	194.44	96.00
295	4	2.11	8.42	163.89	655.56	344.44	96.00
340	4	2.32	9.27	188.89	755.56	244.44	99.00
445	4	2.77	11.08	247.22	988.89	11.11	105.00
450	3	2.79	8.37	250.00	750.00	250.00	106.00

Figure 13: Optimization Study Results: NED Payload Options

4.4. BELASat Design

To reduce the payload mass and minimize the potential points of failure, the BELASat instrument suite is limited to maintaining and maneuvering the NEDs into their detonation positions. An inertial measurement unit (IMU) is responsible for attitude determination and a laser altimeter is used for measuring the distance to the asteroid's surface and acquiring the optimal standoff altitude for NED detonation. The 340 kt NED payload envelope is estimated to be cylindrical with a diameter of 0.5 m and a height of 0.63 m using the heuristic sizing equation from the paper *Conceptual Design of a Flight Validation Mission for a Hypervelocity Asteroid Intercept Vehicle* by Barbee et al. [23]. The nuclear payload sizing envelope is illustrated in Figure 14.

BELASat is designed to be compatible with the ESPA-Grande class satellite bus. The ESPA form factor provides a high TRL common commercial off-the-shelf framework, and the internal ESPA ring houses all power and avionics systems for the MUFN spacecraft bus. The system serves as a compact means of transporting the BELASats, and the deployment system is flight proven to minimize risk during

MUFN operations [24]. After release from the MUFN spacecraft bus, the BELASats rely on a cold-gas reaction control system for attitude control while maneuvering in orbit around 2023 PDC. Nitrogen gas has been selected as the propellant due to its high reliability, ease of storage, and minimized tank mass [25]. 22 cm/s of ΔV is required for all BELASat pre-detonation proximity operations, which includes a 100 percent design margin. Nitrogen has a measured specific thrust of 73 s, and the filled tank is estimated to be 5.73 kg. The 100 percent ΔV margin was included in the design process to allow for deviations from the optimal standoff distance in scenarios where it may be beneficial to impart more or less ΔV onto the asteroid than initially intended. The spare propellant is also allotted to recover from technical issues such as a failed NED detonation. If a BELASat fails to detonate, it will initiate station-keeping operations at the detonation target location. The following BELASat in the detonation sequence will immediately deploy, maneuver to the target location and explode its payload, destroying the malfunctioning satellite.

BELASats will need to sustain operations for three hours from initial deployment to NED detonation. The operating time requirement has been tripled to nine hours for design purposes. Redundant lithium-ion batteries supply power to the satellite and contribute a total mass of 5.2 kg. One BELASat has a wet mass of 249.7 kg and the entire MUFN spacecraft payload mass, consisting of four fully-fueled BELASats, is 998.8 kg.

4.5. Mitigation Method Additional Considerations

4.5.1. Sensitivity in Detonation Standoff Distance

Each BELASat detonation must impart a ΔV equal to or greater than 2.2 mm/s to accomplish requirement **M1** (MUFN shall neutralize the threat posed by 2023 PDC). While each BELASat is designed to detonate at an altitude of 99 m, imparting the maximum ΔV of 2.32 mm/s, there is an acceptable error range of -30 m to +30 meters to achieve successful asteroid deflection. Suppose more ΔV is imparted from a single detonation than initially anticipated. In that case, the standoff detonation can be adjusted to manipulate the ΔV of the subsequent blasts to avoid disruption and achieve the desired design period change. Figure 15 illustrates the imparted ΔV curve with upper and lower error boundaries.

4.5.2. Disruption Considerations

An important consideration when designing a standoff nuclear mitigation mission is ensuring that asteroid disruption does not occur during the detonation, leading to potentially hazardous fragments. Accidental fragmentation could result in multiple fragments of 2023 PDC impacting Earth, making mitigation efforts significantly more difficult, if not impossible. Figure 16 shows the amount of energy (in Joules) per kilogram that would be imparted into 2023 PDC for a range of nuclear devices. In order to ensure that there is no potential for accidental disruption of the asteroid, a heuristic is used to determine that the per unit mass of energy imparted into the asteroid by the nuclear blast shall not exceed 100-1000 J/kg [26]. An assumption made here is that the blast-induced change in kinetic energy of the asteroid is approximately equal to the energy imparted to the asteroid. The 340 kt NED detonations do not exceed this energy requirement, as it is orders of magnitude below the heuristic values of 100-1000 J/kg. Even if all the required nuclear yield to deflect the asteroid by 25 mm/s was detonated at once, there would still be no risk of accidental disruption per the stated heuristic relationship.

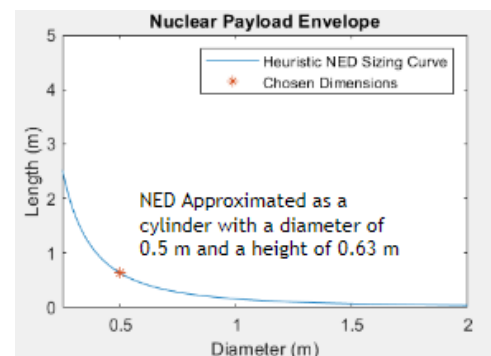


Figure 14: Nuclear Payload Envelope

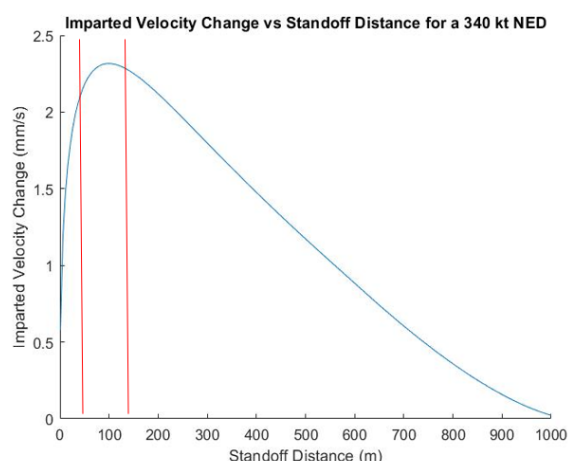


Figure 15: Blast Effectiveness Sensitivity

To avoid disruption of 2023 PDC, verifying that the imparted ΔV from each NED detonation does not exceed 10 percent of the asteroid's escape velocity is important. 2023 PDC has a calculated escape velocity of 561 mm/s, setting the 10 percent maximum requirement at 56 mm/s [27, 28]. The escape velocity plot for 2023 PDC is illustrated in 17. Since the 10 percent escape velocity threshold is over two times the total required ΔV for a successful deflection, there is no risk of disruption [26, 29].

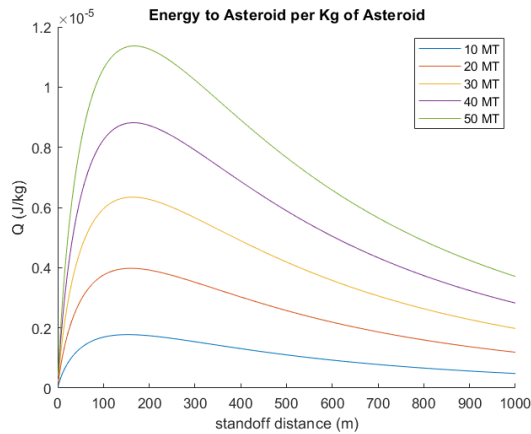


Figure 16: Relationship Between Standoff Distance, Device Yield, and Imparted ΔV

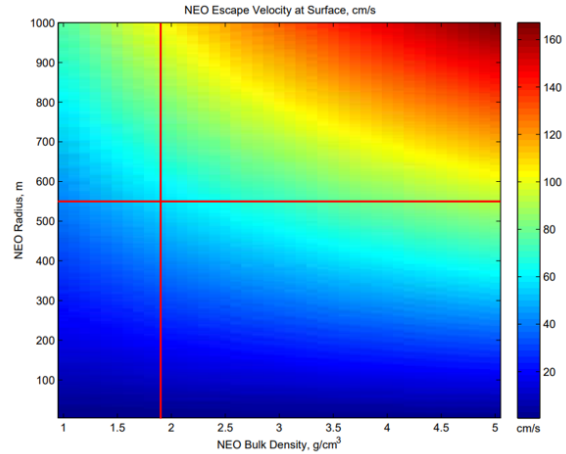


Figure 17: 2023 Escape Velocity Analysis[28]

4.6. MUFN and BelaSat Proximity Operations

The MUFN mitigation mission relies on proximity operations around 2023 PDC to complete the mission. The MUFN bus spacecraft will be station-keeping above the surface of the asteroid. At the same time, each BELASat must enter an elliptic transfer orbit to convey the nuclear device to the intended detonation location. This section will walk through the determination of each spacecraft's proximity operations budgets. Figure 18 details the relative positions of MUFN and each BELASat during the proximity operations phase of the mission.

4.6.1. MUFN Station-keeping

MUFN will be required to station keep above the surface of 2023 PDC. Station-keeping based proximity operations were selected for MUFN to fix the spacecraft's location relative to the asteroid for the duration of its mission. Doing so makes the transfer of the BELASAT easier to construct because there is only one moving object in the vicinity of 2023 PDC. MUFN will conduct its station-keeping on the opposite side of the asteroid from the BELASat detonation position (as shown in 18). It was determined that MUFN will station-keep at an altitude of 1.75 km above the surface of 2023 PDC.

This altitude was selected for two reasons. The first is that the THEO reconnaissance spacecraft will conduct a 1.75 km altitude survey orbit prior to MUFN's arrival, therefore giving high-fidelity orbit information at this altitude. The second is that the fuel required for station-keeping decreases exponentially as station-keeping altitude increases. Therefore, it is favorable to have a higher station-keeping altitude [27]. Figure 19 shows this relationship between required station-keeping fuel and station-keeping altitude. The red vertical line represents the radius of the 2023 PDC, as a spacecraft would not be able to station-keep within the asteroid's radius.

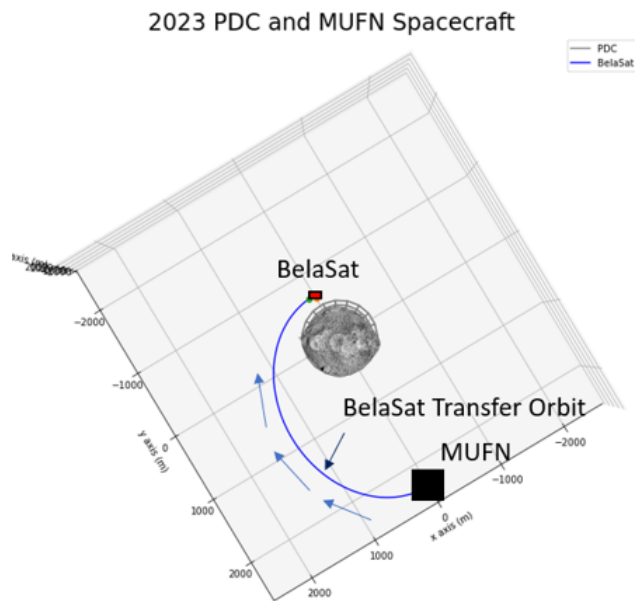


Figure 18: MUFN and BelaSat proximity operations - - orbits to scale, objects not to scale

4.6.2. BelaSat Transfer Orbit

While MUFN is station-keeping 1.75 km above 2023 PDC, an individual BELASat will separate from the MUFN spacecraft every three days and enter a transfer orbit to the intended detonation location. This intended detonation location is 99 meters above the surface of 2023 PDC on the opposite side of the asteroid relative to the station-keeping MUFN spacecraft. Figure 18 depicts this transfer orbit and relative positioning of MUFN and BELASat at the time of detonation. To travel to the intended detonation location, each BELASat will separate from MUFN and immediately enter an elliptic transfer orbit using an impulsive burn from cold gas (nitrogen) thrusters. Using an n-body propagator with solar radiation pressure included and considering the gravity of the Sun and 2023 PDC, it was determined that 0.11 meters per second of ΔV is required per BELASat to successfully enter the detonation transfer orbit.

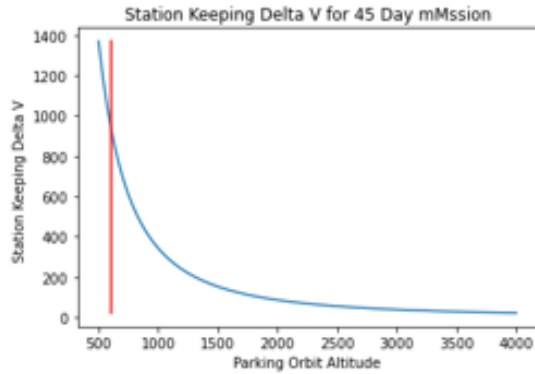


Figure 19: MUFN parking orbit station-keeping altitude vs required ΔV for notional 45 day mission

4.6.3. Overall Station-keeping Budget

Using the discussion above, a nominal station-keeping budget for MUFN and BELASat can be established. Based on the discussion in the Mitigation Assessment Consideration section above, three days are needed to determine the effectiveness of each detonation and allow blast ejecta to clear. Since each MUFN has 4 BELASats attached, a nominal mission lifetime of 12 days is required. Four days of additional mission time margin is added, meaning that each MUFN spacecraft must station-keep at a 1.75 km altitude above 2023 PDC for 16 days. This translates to a station-keeping ΔV requirement of 24 m/s. Twenty percent additional station-keeping ΔV margin will be added to account for any unexpected but necessary maneuvers (such as debris avoidance). This places a 32 m/s ΔV budget on the MUFN spacecraft. As discussed previously, each BELASat transfer maneuver will require 0.11 m/s of ΔV . A 100 percent ΔV margin will be added to account for orbit corrections or unexpected maneuvers. This places a 0.22 m/s ΔV budget on each BELASat.

4.7. Spacecraft Design

The MUFN spacecraft will consist of several subsystems assembled around a vertical truss and wrapped in insulatory material. Figure 20 details the arrangement of the BELASats around the MUFN spacecraft; the entire assembly fits easily within a Falcon Heavy standard fairing. A mass and power summary for the MUFN subsystems is provided in Table 9.

Table 9: MUFN subsystem mass overview

MUFN Subsystem	Primary Components	Mass (kg)	Power (W)
Power	RTG (2)	114	600 (provided)
Propulsion (dry)	Thrusters, Engine, Tanks	267	222
Thermal	Radiators, Mylar blankets	30	100
Separation	4x RocketLab mkII Motorized Lightbands	40	30
Communications	2x Omni antenna, 1x 2m HGA	69	188
Guidance and Navigation	Camera, IMU, Star tracker, sun tracker, computer	8	30
TOTAL		528	500

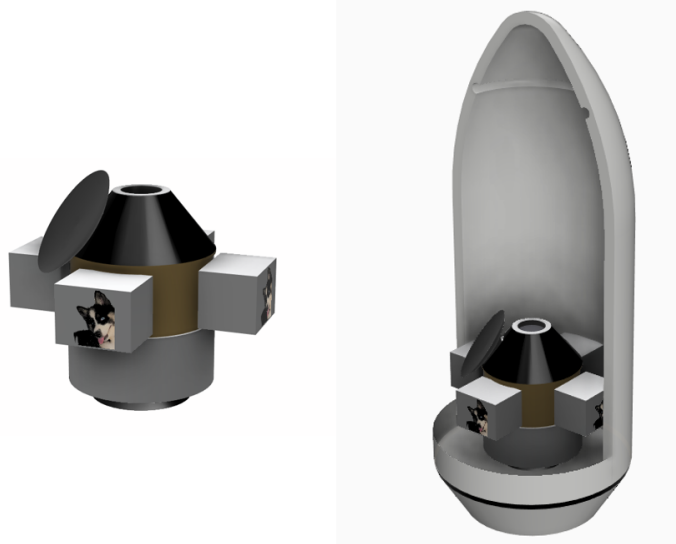


Figure 20: MUFN Spacecraft Assembly and Integration into Falcon Heavy Standard Payload Fairing

The power source for the MUFN and BELASat spacecraft system will consist primarily of 2 RTGs. RTGs were selected for the MUFN spacecraft instead of the solar panels used on THEO due to the potential of asteroid ejecta interfering with the solar panel's performance during detonation events. Using an RTG nullifies the need for deployable structures on the MUFN spacecraft bus. As discussed in previous sections, each BELASat will be powered by Lithium-Ion batteries. These batteries will be trickle charged from MUFN's RTGs.

The propulsion system will be a hypergolic single-engine system utilizing monomethylhydrazine (MMH) and mixed oxides of nitrogen with 25 percent nitric oxide (MON25). There will be an additional engine as a backup with redundant plumbing and valves. The main engine will be a derivative of the Aerojet Rocketdyne R-42 and will provide approximately 900 N of thrust. The R-42 will be altered to increase the expansion ratio, improve specific impulse in a vacuum (340s target), and optimize the adjustment from MON3 to MON25. The decision to use MON25 instead of MON3 or nitrogen tetroxide (NTO) is based on the interplanetary space temperature. The combination of oxidizer and propellant is storable in the solar orbit environment and provides a lower freezing temperature than hydrazine with a better specific impulse. [30] This cold propulsion operation condition will reduce thermal heating requirements for the fuel and main engines.

The system will have a maximum capacity of 3000 kg of propellant and oxidizer; the MON25 and MMH are contained at a 1.5 to 1 ratio by mass. There are two tanks for the propellant, two for the oxidizer, and two for the helium that maintains system pressure. The system has no pumps and uses valves and pressure for the combustion reaction. The attitude control system will utilize eight Aerojet Rocketdyne MR-103J 1N hydrazine monopropellant-catalyst pulsed thrusters and eight backups. The thrusters will be arranged in a cross configuration that provides yaw, pitch, and roll control. 100 kg of hydrazine is stored between 4 spherical tanks above the propellant and oxidizer tanks. The 3000 kg capacity across all four fuel tanks will enable three 21-day launch periods in a row. Based on this design, the spacecraft may require much less than 3000 kg for some of the launch days, but at the edges of the extended period, it requires 3000 kg. Depending on the launch day, the vehicle will be launched with between 1200kg and 3000kg of propellant. This will be expanded upon further in the MUFN trajectory analysis.

4.8. Launch Vehicle, Trajectory, and Mission Performance

A study of potential Earth launch and 2023 PDC arrival dates were investigated alongside various times-of-flight (TOF) using a Type II Lamberts solution. Launch dates from 01/01/2028 to 01/01/2030 and arrival dates from 02/01/2028 to 11/22/2032 were considered. The trajectory search was further constrained by considering missions with C_3 estimates less than $70 \text{ km}^2/\text{s}^2$. In this section, C_3 refers to the performance requirement for the launch vehicle and Δv refers to the asteroid arrival performance required of the spacecraft. The launch vehicle requirements can be identified based on these initial trajectory characteristics.

4.8.1. Launch Vehicle

Several commercial launch vehicles can deliver a spacecraft with a maximum mass of 5000 kg to orbit. However, only the expendable Falcon Heavy can provide the necessary performance for this mission[31]. The range of C_3 and DLA values for this mass requirement makes it unlikely that any other existing commercial launch vehicle will provide the required performance. The Falcon Heavy Expendable performance has been incorporated into the system model via a lookup table. This lookup table interpolates on performance data [31] and applies a variable DLA penalty if the vehicle trajectory is between 28.5 and 57 degrees.

4.8.2. Spacecraft Model and Navigation Solutions

A rocket performance model was constructed to refine the trajectory characterization further. The model incorporated all the subsystem mass estimate models, the payload mass, the launch vehicle performance model, the spacecraft engine performance model, and the trajectory characteristics for every specific launch day, arrival day, departure direction, and several revolution combinations. The design was iterated based on the maximum propellant tank capacity. This design included a minimum mass margin of 20% for the spacecraft and launch vehicle. The 3000 kg fuel tank model was selected to minimize mass but maintain three consecutive 21-launch-day periods. The model was run with the 3000 kg maximum propellant mass design; this resulted in an array of launch and arrival dates that were viable for the design architecture. Figure 21 defines an area of the parameter space where launches are viable. An optimization strategy selected the specific launch trajectory for each day from this parameter space. This strategy determined the maximum mass error margin for each launch date and down-selected a single trajectory based on maximizing that metric. This strategy selected trajectories that maximized robustness against launch vehicle and spacecraft performance error.

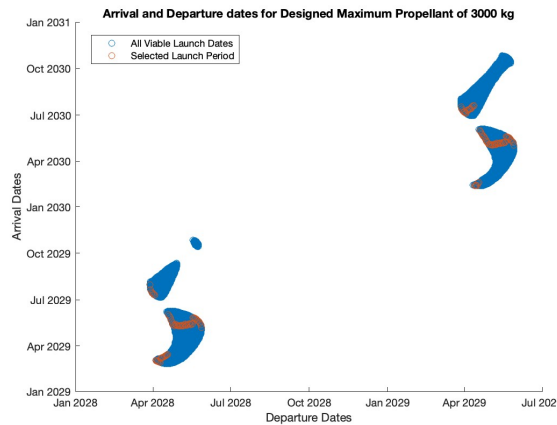


Figure 21: MUFN Viable Arrival and Departure Dates

The visual representation of the arrival and departure dates suggests a primary and a backup launch year based on the ability to have three launch periods consecutively each year. The primary launch periods will start on 03/28/2028 and end on 05/28/2028. The backup launch periods will start on 03/28/2029 and end on 05/29/2029. Table 10 lists examples of launch and arrival date characteristics. Specifically, it provides the first day of each launch period with the performance error margin optimized arrival date and trajectory.

Table 10: MUFN Trajectories for the First Launch Day in each Launch Period

Launch Date	Arrival Date	TOF [Days]	Launch C_3 [km^2/s^2]	ΔV [km/s]	DLA [degrees]
03/28/2028	07/30/2029	489	40.3	3.6	32.1
04/17/2028	03/14/2029	331	30.8	3.0	56.9
05/07/2028	05/11/2029	369	19.7	2.6	51.1
03/28/2029	07/17/2030	476	33.2	3.6	30.5
04/17/2029	02/17/2030	306	29.6	3.4	56.9
05/07/2029	05/04/2030	362	20.4	2.4	54.3

The trajectory characteristics and vehicle performance for the primary and backup launch periods are provided in Figures 22, 23, 24, and 25. These plots characterize three launch periods in a row for the primary and backup launch years. The launch periods align like this due to the orbital dynamics between Earth and 2023 PDC. Figure 22 provides the primary launch period C3, DLA, and Δv . The primary launch period mass budget and margin for the mission are contained within Figure 23. The spacecraft propellant mass fluctuates because the trajectory selected may not require a full tank of propellant and the launch vehicle requires a lighter payload in order to achieve the highest performance margin. The performance error margins are optimized to be as high as possible and are never below 20%. The spacecraft mass never crosses 4600 kg, which is below the **M4** requirement. In the primary period the launch vehicle is most stressed prior to the DLA maxing out. After that, the performance margin increases substantially. Figure 24 contains the backup launch period C3, DLA, and Δv , and Figure 25 contains mass budget and margin for the mission. The backup launch period shows similar behavior to the primary launch period with similar performance margin.

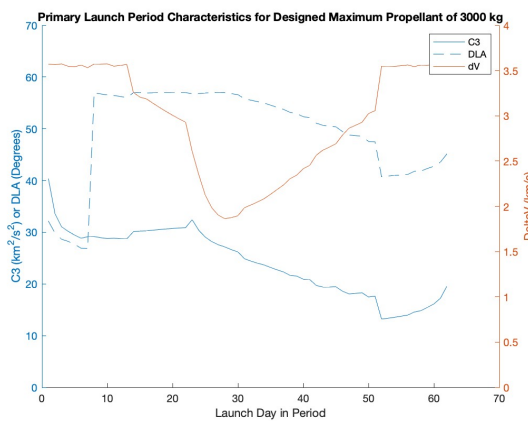


Figure 22: Primary Launch Period Performance Characteristics

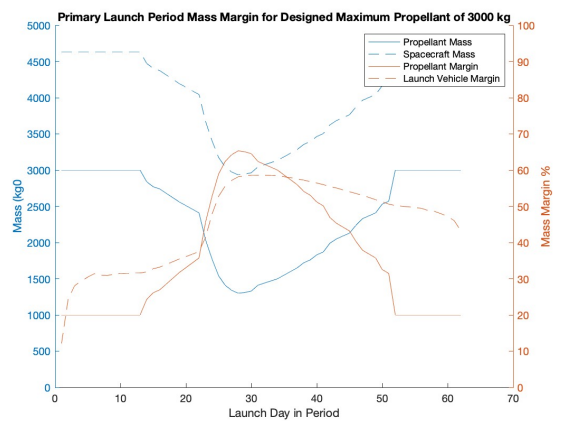


Figure 23: Primary Launch Period Mass Characteristics

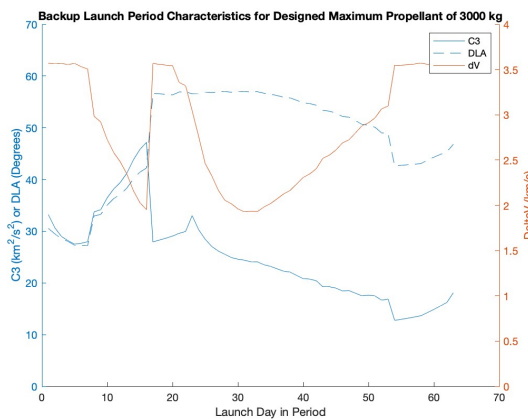


Figure 24: Backup Launch Period Performance Characteristics

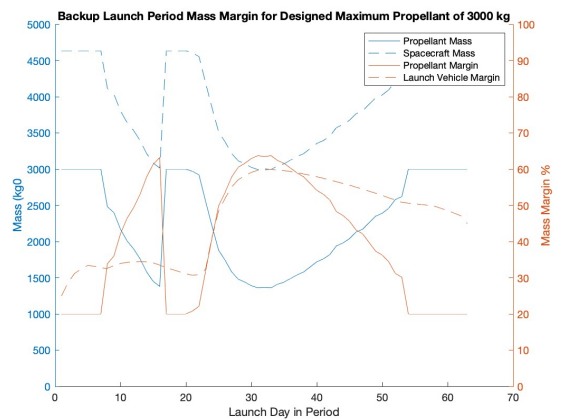


Figure 25: Backup Launch Period Mass Characteristics

4.8.3. Deep Space Maneuvers

A total of 3 deep space maneuvers will be completed prior to rendezvous. These maneuvers are intended to slow the vehicle down as it arrives and provide time to identify issues if they arise during the terminal phase of the trajectory. Table 11 provides the times each maneuver will be performed and includes the approximate burn times and Δv of the maneuvers. Note that the burn times and Δv are based on the launch trajectory used to deliver MUFN to 2023 PDC. So these will vary based on the launch date and optimization method selected for that particular launch. The values listed contain the parameter space of all possible launches shown in Figure 21.

Table 11: Deep Space Maneuvers

Trajectory Description	Transfer Time	Burn Time (min)	Δv (km/s)
Deep Space Maneuver 1	2 weeks prior to intercept	20-40	1.0-2.0
Deep Space Maneuver 2	2 days prior to intercept	10-20	0.5-0.75
Deep Space Maneuver 3	2 hours prior to intercept	8-17	0.5-0.75
Arrival Maneuver	10 minutes prior to intercept	1	0.1

4.8.4. Detonation Dates and Performance

Depending on the launch date and trajectory, the spacecraft could arrive at 2023 PDC on different dates. If a backup launch needs to be used, the spacecraft will arrive about a year later than predicted. A simulation of deflection based on the date was created for NED sizing validation. This simulation applies the Δv of each NEDs in a single impulse antiparallel to the velocity vector and then propagates 2023 PDC past Earth impact; Figure 26 shows the results of this simulation. The simulation indicates that it is always better to decelerate 2023 PDC than accelerate it relative to the velocity vector. It also confirms that there are better times to detonate the NEDs depending on the orbital characteristics of 2023 PDC at the time of detonation. These ideal detonation times have been identified, and the NEDs will wait to detonate if there is a higher impact detonation time in the future. Thus the arrival date of a MUFN spacecraft at 2023 PDC is not necessarily the first detonation date.

Figure 27 is a simulation of the detonations based on the launch and arrival dates of MUFN to 2023 PDC. It only simulates 3 MUFN launches at the beginning of each of the six launch periods. This simulates failure to launch or failure in flight. The worst-case scenario for this mission is all three MUFN spacecraft launching in the backup launch period. Backup 3 shows a near miss at just above 1500 km altitude if this occurs. If the first three launch periods are successfully used, then 2023 PDC is projected to pass by Earth at about 3500 km altitude. A substantial margin is built into this mission; the margin is built into the spacecraft mass, launch vehicle mass delivery performance, and required detonation dates. The mission can be 20% over mass budget, miss the first 3 of 6 launches, and still achieve success. If THEO discovers 2023 PDC to be a more challenging target than the 90th percentile parameters, then the three backup launch periods can be used to supplement the quantities of NEDs being delivered to the asteroid.

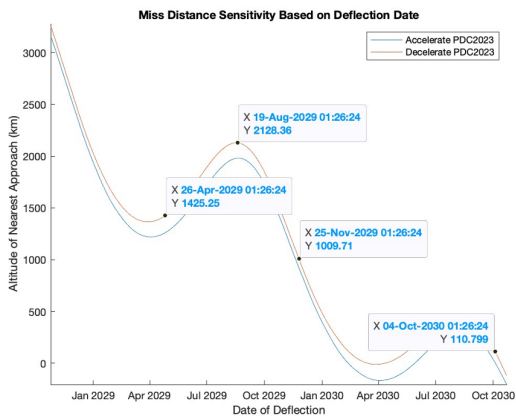


Figure 26: Miss Distance Sensitivity

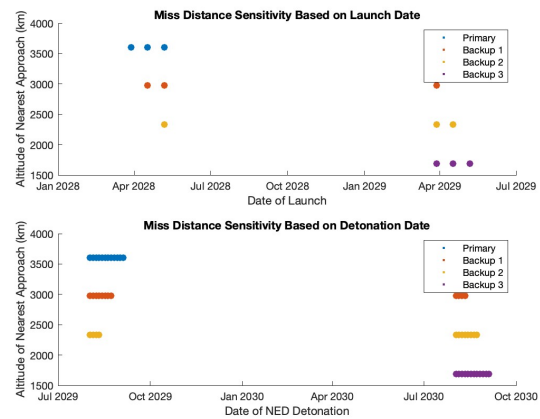


Figure 27: Mitigation Mission Performance

5. Expected Mission Outcome

A mission of this degree of complexity requires measured risk-taking. A risk stoplight chart is presented in Figure 28 to assist in identifying the major mission risk areas. The risk stoplight chart aims to identify risk mitigation methods early in the design process.

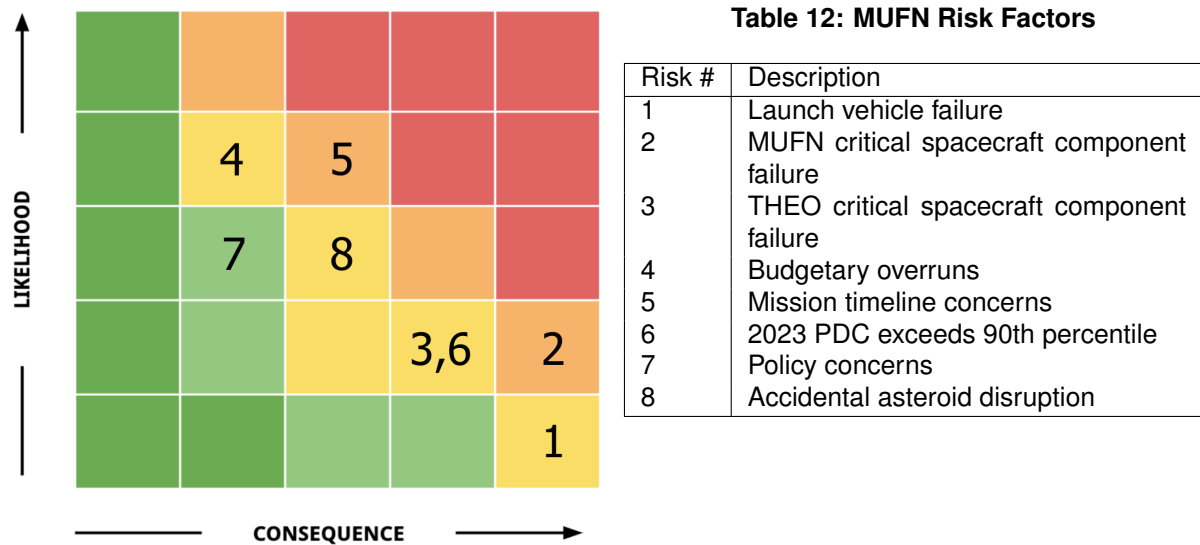


Figure 28: Program risk areas as a function of likelihood and perceived mission impact

The reconnaissance and mitigation mission hardware are proposed to be made more similar to address risk areas 4 and 5 (timeline and budgetary issues). Design considerations will be made to reuse technology and design parameters between the two spacecraft. This would reduce the research and development costs for the entire program, allow for a learning curve cost reduction from the first spacecraft to the second, and reduce the time needed for the development of each spacecraft.

Selecting a nuclear standoff detonation as the mitigation method addresses risk areas 3 and 6. Suppose the asteroid exceeds the 90th percentile or higher fidelity data regarding its physical characteristics are unavailable due to the failure of the THEO mission. In that case, the nuclear mitigation option is the most robust mitigation method. The quantity of NEDs can be changed with relative ease compared to responding to changes with other mitigation methods. Risk area 8 is vital to consider, especially concerning risk area 3. If THEO fails, uncertainty regarding 2023 PDC's physical parameters will still be significant. This increases the risk of accidental asteroid disruption due to the mitigation mission.

The MUFN spacecraft will only use components with high TRL to mitigate risk area 2. This will likely require significant development time and funding to increase the TRL for the nuclear detonation device. Risk area 7 will be mitigated by engaging national policy experts and lawyers early in the design process to ensure all policy and legal roadblocks regarding launching a nuclear device into space can be overcome.

Based on the 2023 PDC impact timeline, this development cycle will need to be expedited compared with a more nominal mission timeline. The team is expected to launch THEO in 2025 (2 years after 2023 PDC discovery), and the spacecraft will rendezvous with 2023 PDC in 2026. Within months, THEO is expected to confirm a carbonaceous asteroid and clarify the body's dynamics. Throughout the development of THEO a parallel mission, MUFN, will be in progress to prepare nuclear devices for deep space flight. Three of these devices will be launched in 2028 and rendezvous in 2029. They will provide enough ablation of the surface of 2023 PDC to divert it off the collision course seven years before impact. THEO will observe the detonations from a safe distance and assist in the confirmation of the deviation of 2023 PDC. In 2036 PDC 2023 will pass by Earth at an altitude above 3500 km.

References

- [1] NASA, CNEOS Discovery Statistics, <https://cneos.jpl.nasa.gov/stats/totals.html>, Accessed: 09-13-2022.
- [2] ESA, Near-Earth Objects Risk List, <https://neo.ssa.esa.int/risk-list>, Accessed: 09-13-2022.
- [3] T. Wackler, C. Kontos, J. Wilmer, L. Johnson, A. Pirdgeon, et al., National Near-Earth Object Preparedness Strategy and Action Plan, National Science & Technology Council 23 (2018).
- [4] A. Liakos, A. Bonanos, E. Xilouris, D. Koschny, I. Bellas-Velidis, P. Boumis, V. Charmandaris, A. Dapergolas, A. Fytisilis, A. Maroussis, et al., NELIOTA: Methods, statistics, and results for meteoroids impacting the Moon, *Astronomy & Astrophysics* 633 (2020) A112.
- [5] A. McEwen, I. Daubar, B. Ivanov, J. Oberst, R. Malhotra, Y. JeongAhn, S. Byrne, Current Impact Rate on Earth, Moon, and Mars (2015).
- [6] NASA, NASA Probe Counts Space Rock Impacts on Mars, <https://www.jpl.nasa.gov/news/nasa-probe-counts-space-rock-impacts-on-mars>, Accessed: 09-29-2022.
- [7] S. Hergarten, T. Kenkmann, The number of impact craters on Earth: Any room for further discoveries?, *Earth and Planetary Science Letters* 425 (2015) 187–192.
- [8] NASA, CNEOS Hypothetical Impact Scenarios, <https://cneos.jpl.nasa.gov/pd/cs/pdc23/>, Accessed: 12-18-2022.
- [9] M. G. Schaffer, A. Charania, J. R. Olds, Evaluating the effectiveness of different NEO mitigation options, in: 2007 Planetary Defense Conference.
- [10] L. Prockter, S. Murchie, A. Cheng, S. Krimigis, R. Farquhar, A. Santo, The NEAR Shoemaker Mission to Asteroid 433 Eros, *Acta Astronautica* 51 (2002) 491–500.
- [11] C. Russel, F. Capaccioni, A. Coradini, M. De Sanctis, W. Feldman, R. Jaumann, H. Keller, T. McCord, L. McFladden, S. Mottola, C. Pieters, T. Prettyman, C. Raymond, M. Sykes, D. Smith, M. Zuber, Dawn Mission to Vesta and Ceres: Symbiosis between Terrestrial Observations and Robotic Exploration, *Earth Moon Planet* 101 (2007) 65–91.
- [12] K. Glassmeier, H. Boehnhardt, D. Koschny, E. Kürt, I. Richter, The Rosetta Mission: Flying Towards the Origin of the Solar System, *Space Science Reviews* 128 (2007) 1–21.
- [13] W. Hart, G. M. Brown, S. M. Collins, M. De Soria-Santacruz Pich, P. Fieseler, D. Goebel, D. Marsh, D. Y. Oh, S. Snyder, N. Warner, G. Whiffen, Elkins-Tanton, Overview of the spacecraft design for the Psyche mission concept, in: 2018 IEEE Aerospace Conference, IEEE, Big Sky, MT, 2018, pp. 1–20.
- [14] R. A. Masterson, M. Chodas, L. Bayley, B. Allen, J. Hong, P. Biswas, C. McMenamin, K. Stout, E. Bokhour, H. Bralower, D. Carte, S. Chen, M. Jones, S. Kissel, F. Schmidt, M. Smith, G. Sondecke, L. F. Lim, D. S. Lauretta, J. E. Grindlay, R. P. Binzel, Regolith X-Ray Imaging Spectrometer (REXIS) Aboard the OSIRIS-REx Asteroid Sample Return Mission, *Space Science Reviews* 214 (2018) 48.
- [15] B. Rizk, C. Drouet d'Aubigny, D. Golish, C. Fellows, C. Merrill, P. Smith, M. Walker, J. Hendershot, J. Hancock, S. Bailey, et al., OCAMS: the OSIRIS-REx camera suite, *Space Science Reviews* 214 (2018) 1–55.
- [16] M. G. Daly, O. S. Barnouin, C. Dickinson, J. Seabrook, C. L. Johnson, G. Cunningham, T. Haltigin, D. Gaudreau, C. Brunet, I. Aslam, A. Taylor, E. B. Bierhaus, W. Boynton, M. Nolan, D. S. Lauretta, The OSIRIS-REx Laser Altimeter (OLA) Investigation and Instrument, *Space Science Reviews* 212 (2017) 899–924.
- [17] T. Mukai, H. Araki, T. Mizuno, N. Hatanaka, A. M. Nakamura, A. Kamei, H. Nakayama, A. Cheng, Detection of Mass, Shape and Surface Roughness of Target Asteroid of MUSES-C By LIDAR, *Advance Space Research* 29 (2002) 1231–1235.
- [18] J. Kreitzman, C. W. Stewart, E. Cansler, J. Brisby, M. Green, J. Lyne, Mission Opportunities to Trans-Neptunian Objects—Part III, Orbital Capture, Low-Thrust Trajectories and Vehicle Radiation Environment During Jovian Flyby, *Advances in the Astronautical Sciences* 150 (2013) 1487–1506.
- [19] B. Wie, Astrodynamics fundamentals for deflecting hazardous near-earth objects, in: 60th International Astronautical Congress, IAC-09-C1, volume 3, p. 12.
- [20] NASA, Nuclear Weapon Effects in Space, <https://history.nasa.gov/conghand/nuclear.htm>, Accessed: 03-19-2023.
- [21] NASA JPL, NASA/JPL NEO Deflection App, <https://cneos.jpl.nasa.gov/nda/nda.html>, Accessed: 10-03-2022.
- [22] R. Managan, J. Wasem, K. Howley, Near Earth Object Deflection Formulae, Technical Report, Lawrence Livermore National Lab.(LLNL), Livermore, CA (United States), 2021.
- [23] B. Barbee, B. Wie, M. Steiner, K. Getzandanner, Conceptual design of a flight validation mission for a Hypervelocity Asteroid Intercept Vehicle, *Acta Astronautica* 106 (2015).
- [24] J. R. Maly, M. E. Evert, J. T. Shepard, C. A. Smith, Space access for small satellites on rideshare missions with ESPA and ESPA-derived payload adapters, in: 2011 Aerospace Conference, IEEE, pp. 1–8.
- [25] A. Anis, Cold gas propulsion system-an ideal choice for remote sensing small satellites, in: B. Escalante-Ramirez (Ed.), *Remote Sensing: Advanced Techniques and Platforms*, InTech, 2012, pp. 447–462.
- [26] B. Barbee, Lecture 7: Overview of NEO Deflection and Disruption, 2022. ENAE603 - Near-Earth Object Exploration.
- [27] D. Vallado, W. McClain, *Fundamentals of Astrodynamics and Applications*, Space technology library, Microcosm Press, 2013.
- [28] B. Barbee, Lecture 11: Introduction to Spacecraft Motion in Proximity to NEOs, 2022. ENAE603 - Near-Earth Object Exploration.
- [29] B. Barbee, Lecture 5: Overview of Interplanetary Trajectory Concepts, 2022. ENAE603 - Near-Earth Object Exploration.
- [30] H. P. Trinh, C. Burnside, H. Williams, Assessment of MON-25/MMH Propellant System for Deep-Space Engines, in: International Astronautical Congress (IAC), M19-7648.
- [31] NASA, NASA Launch Services Program (LSP) Performance, <https://elvperf.ksc.nasa.gov/Pages/Default.aspx>, Accessed: 10-03-2022.